

However, the onset of instabilities and chaos in these laser systems requires not only a bad-cavity condition but also a gain considerably above lasing threshold. Attention has been given identifying lasers that use transitions such that the resonator and the medium decay rates can satisfy the bad-cavity condition and the high gain. Perhaps, the optically pumped NH₃ far-infrared laser is the most promising candidates in this regard (Harrison and Al-Saidi 1985, Harrison, et al. 1985. Al-Saidi and Mahdi, 2005). The signal-mode semiconductor laser is also a good example of laser that satisfies the condition for optical instabilities and can easily display different types of pulsations and chaotic behaviors (Yao et al. 1995, Van Tarwijk and Agrawal 1998).

The originally (classical) Lorenz-Haken equations are based on a two-level homogeneously broadened laser system with a symmetric Lorentzian gain profile. In order to investigate the effects of the asymmetry of the gain profile and inhomogeneous broadening on the dynamics of the laser system, two additional parameters are introduced into these equations. The resulting generalized Lorenz-Haken equations were used to study the dynamics of the signal-mode semiconductor laser (Yao, et al. 1995).

The purpose of this paper is to investigate the effects of the additional parameters (α and θ) on the dynamical behaviors of the laser system based on the generalized Lorenz-Haken based on the generalized Lorenz-Haken equations (Weiss and Vilaseca 1991).

Theoretical Considerations

The generalized Lorenz-Haken equations can be written in the following form:

$$\dot{x} = -\sigma(x - y) \quad (1)$$

$$\dot{y} = -(1 + i\alpha)[y - (1 - i\theta)(r - z)x] \quad (2)$$

$$\dot{z} = -bz + \text{Re}(x^* y) \quad (3)$$

Where $\sigma = k/\gamma_{\perp}$, $b = \gamma_{\parallel}/\gamma_{\perp}$, and r is the pump parameter, and the variables x , y , z are proportional to the amplitudes of the electric field, atomic polarization, and population inversion, respectively with corresponding decay rates k , γ_{\perp} , and γ_{\parallel} .

The two parameters α and θ are new controlling parameters, where α controls the coupling between the amplified and the phase variations (sometimes called line width enhancement factor, which is

related to the medium refractive index) and θ controls the inhomogeneous broadening of the resonance of the resonance. It should be noticed that when we set $\alpha = \theta = 0$ in Eq. (2), the generalized Lorenz-Haken equations reduce to the well-known standard (or classical) Lorenz-Haken equations (H. Haken, 1975, R. Graham, 1976). Re and (*) in Eq. (3) are denoting the real part and the complex conjugate, respectively.

Results and Discussion

For studying the dynamical behaviors of the laser system that satisfy the bad-cavity condition ($\sigma > b + 1$), we have set $\sigma = 3$, $b = 1$. Also, in order to achieve the instability threshold (namely, the pump value at which the laser output becomes unstable), we have taken the pump parameter value $r = 21$ (i.e., 21 times the lasing threshold for laser system). We have numerically solved the Lorenz-Haken equations (1) – (3) for selected values of the control parameters a and θ using the standard fourth-order Runge-Kutta method.

Fig.1 illustrates the effect of variation the parameter a on the dynamical behavior of the laser system, when $\theta = 0$. the value of a changed over the selected range $\alpha = 0.20 - 0.05$. The left column represents the laser output intensity ($|x|^2$) as a function of times, while the right column represents the phase-space portrait (the laser output intensity ($|x|^2$) versus the population inversion (z) corresponding to the time - series in the left column. We notice that our laser systems persisting to follow the well known universal route to chaos, the so-called period - doubling route (or Feigenbaum scenario) (Feigenbaum, 1979, Cvitanovic 1984). In Fig.1 (a), we note that the laser system exhibits stable periodic pulsations of period one, and the corresponding phase - space trajectory is a single limit cycle as shown in Fig.1 (b). This behavior changes to pulsations with period two when α reduces to $\alpha = 0.1$ (Fig.1 (c)) and this leads to a system trajectory with two cycles, as shown in Fig.1 (d). As α is reduced further ($\alpha = 0.080, 0.076, 0.050$), more bifurcations appear these are period - four pulsations, period - eight pulsations (Fig.1 (e) and (g) and the sequence transitions end by appearing of chaotic state as shown in Fig.1 (I). The corresponding attractor trajectories (orbits) are shown in Fig.1. (f), (h), and (j), respectively, where four cycles, eight cycle, and many cycles pattern produce cause the system to become chaotic. It is clearly seen that when $\alpha = 0.050$, the laser system displays irregular pulsations which are the nature of the chaotic behavior.

In order to have more information about our laser system, we plotted the imaginary part of the laser field amplitude ($\text{Im}(x)$) versus the real part of the laser filed amplitude ($\text{Re}(x)$) and also we have plotted the power (or

intensity) spectrum corresponding to the time-series. These are shown in Fig.2, where the left column represents the laser filed intensity picture, while the right column represents the power spectrum. It is clearly evident that when the system exhibits stable periodic pulsations, single frequency (single peak) appears in the power spectrum plot (as we can see in Fig.2.(b)), and two distinguished frequencies appear when the laser output is a period-two pulsations (as shown in Fig.2.(d)). Sequence of additional frequency peaks appear as the doubling of the period of the pulsations train continues, as shown in Fig.2 (f) and (h) until the system reaches the chaotic state as in Figs.2 (j), where the spectrum becomes a broad band which is the main characteristic of the chaotic behavior.

To provide clear picture of the dynamic of laser system and learn more from the instabilities of our present work we have examined the effects of varying the control parameters θ , when α sets to zero ($\alpha = 0$). We have varied θ over the selected range $\theta = 0.15 - 0.03$, we have obtained qualitatively similar behaviors (results) to the case of varying α (i.e. Fig.1) but with different parameter values. Fig.3 and Fig.4 illustrate the results obtained from this investigation.

When we tried to vary the values of the parameters α and θ by the same amount (i.e., $\alpha = \theta$), we obtained similar results to the preceding ones. The path leading to chaos in the laser system again follows Feigenbaum's scenario. The representative examples for such behaviors when $\alpha = \theta$ (= 2.0-0.1) are illustrated in Figs. (5) and (6). The results obtained give an indication that our system transfers into chaotic attractor (chaos) regime only via a period - doubling sequence (route). It is interesting to note that our system can be nicely controlled over a range of laser operating conditions simply (just) by decreasing (or increasing) the values of the system control parameters.

Conclusion

We have investigated the effect of the main control parameters on the dynamical features of the modified Lorenz-Haken laser system. We have observed period - doubling bifurcations and chaos. The results obtained using this simple mathematical model established the suitability of the Lorenz-Haken system for studying the dynamical behavior of the laser system, because of the variations of the main system control parameters capable to achieve a controllable instabilities in the laser system.

References

Al-Saidi I.A and Mahdi F.A, "Nonlinear Dynamic Features of NH3–FIR Laser System" , Basrah J. Sci. (to be published 2005).

- Arecchi F. T. (1987), " Instabilities and Chaos in Signal-mode Homogeneous Line Lasers ", *Instabilities and Chaos in Quantum Optics*, Eds. Arecchi F. T. and Harrison R. G. (Springer Verlag, Berlin, Heidelberg, 1987).
- Arecchi F. T. (1988), " Instabilities and chaos in laser " : Introduction to Hyper chaos (IC Corso, Soc. Italiana di Fisica-Bolognd-italy).
- Arecchi F. T., Lippi G. L., Puccioni G.P, and Terdicce J.R. (1984), " Route to Chaos in a Co2 Laser with injected Signal " , *Opt.Commun.* 51,308.
- Cvitanovic P. (Ed.) (1984), " University of Chaos " , (Adm-Hilger , Bristol).
- Feigenbaum M. J. (1980), " Universal Behavior in Nonlinear System " , *Los Alamos Sci.* 1, 4.
- Grahm R. (1976), " Onset of Self-Pulsing in laser and the Lorenz Model " , *Phys. Lett* 58A, 440.
- Haken H. (1975), " Analogy Between Higher Instabilities in Fluids and Laser " , *Phys. Lett* A53, 77.
- Harrison R. G. and Al-Saidi I. A. (1985), " Experimental Evidence of Self-Pulsing and Chaos in an Optically Pumbed 12 μ m NH₃ Laser " , *Opt.Commun.* 54, 107.
- Harrison R. G., Al-Saidi I. A., and Biswas D. J. (1985), " Observation of Instabilities and Chaos in a Homogeneously Broadened Signal Mode and Multimode Midinfrared Raman Laser " , *Special Issue of IEEE. J. Quantum Electronics*, QE-21, 491.
- Lorenz E. N. (1963), " Deterministic Nonperiodic Flow " , *J. Atoms. Sci.* 20 , 130 Van Trawijk G.H.M. and Agrawal G.P. (1988), " Laser Instabilities a Modern Perspective " , *Prog. Quantum Electron.*, 22 , 43.
- Weiss C. O. and Klische W. (1984), " Observability of Lorenz Instabilities in Laser " , *Opt. Commun.*, 51 , 47.
- Weiss C. O. and Vilaseca R. (1991), " Dynamics of Lasers " , (VCH. Weinheim).
- Yao J., Agrawal G. P., Gallion P., and Bowden C. M. (1995), " Dynamics of Single-mode Semiconductor Laser " , *Opt.Commun.*, 119, 246.

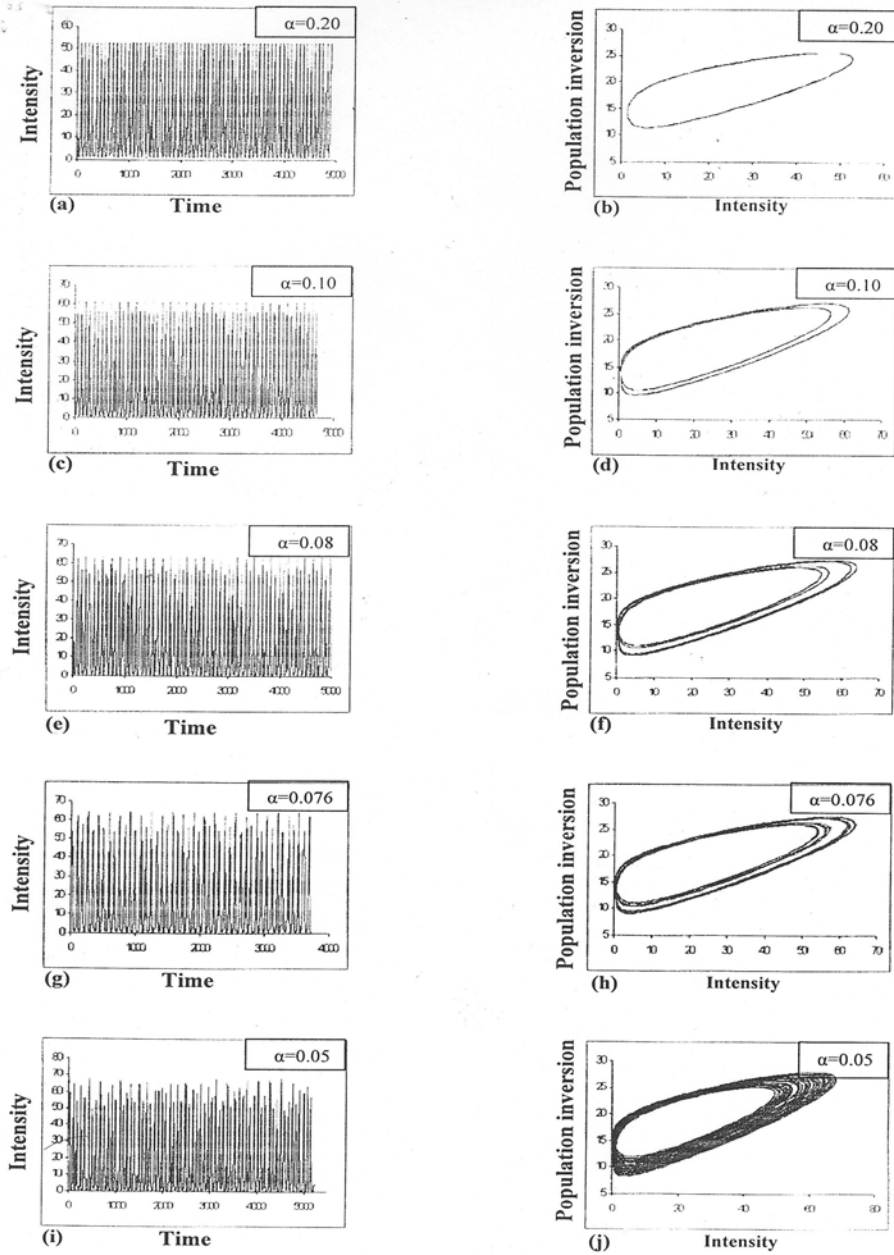


Fig.1

Fig.1. Left Column : Time-series (normalized laser field intensity ($|x|^2$) versus normalized time) at $r = 21$, $\sigma = 3$, $b = 1$, and $\theta = 0$ For different values of α . Right column : The corresponding Phase-space portrait (laser field intensity versus population inversion).

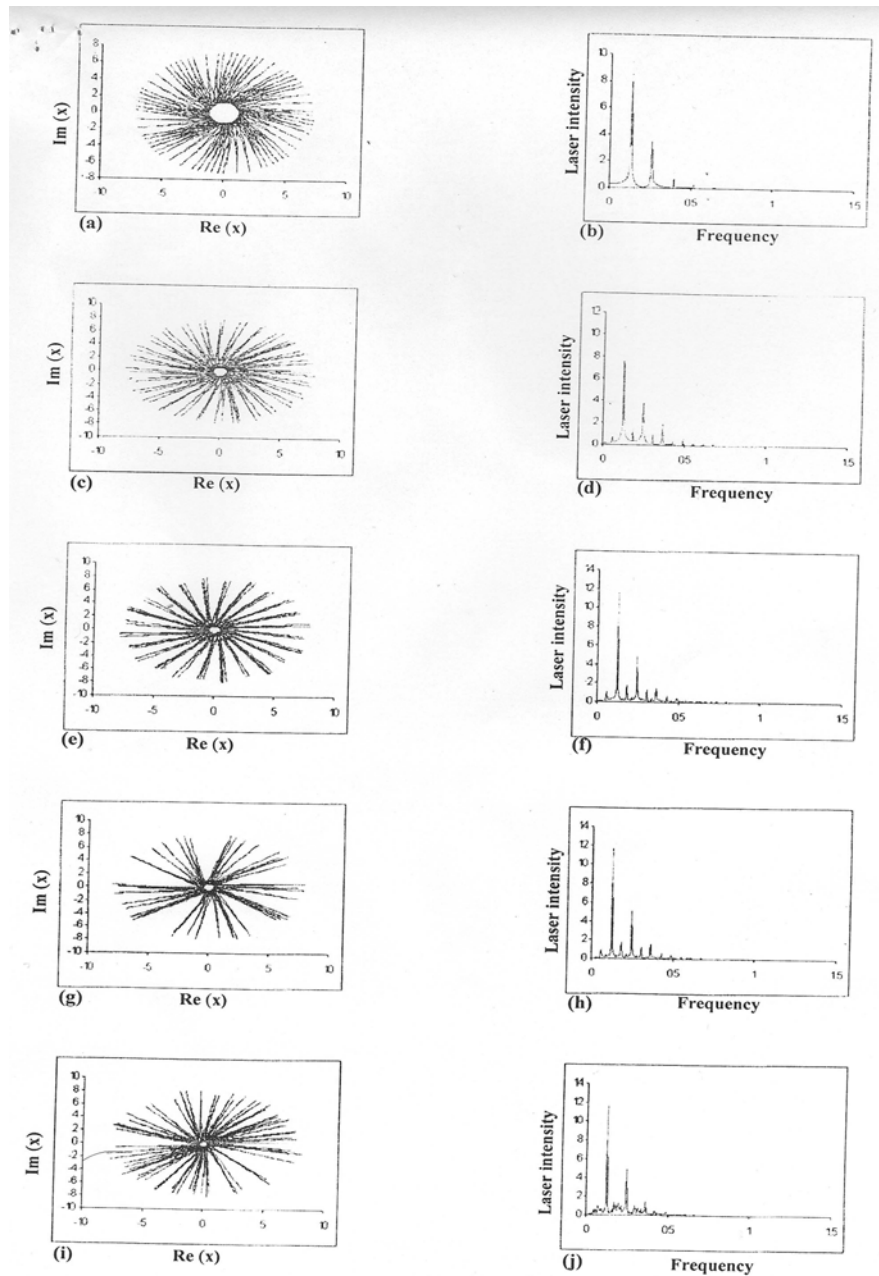


Fig.2

Fig.2. Left column : Imaginary part of the laser field amplitude ($\text{Im}(x)$) as a function of the real part of laser field amplitude ($\text{Re}(x)$) corresponding to Fig.1.
 Right column : Power spectra (normalized laser field intensity versus normalized frequency) corresponding to the time-series plots in Fig.1.

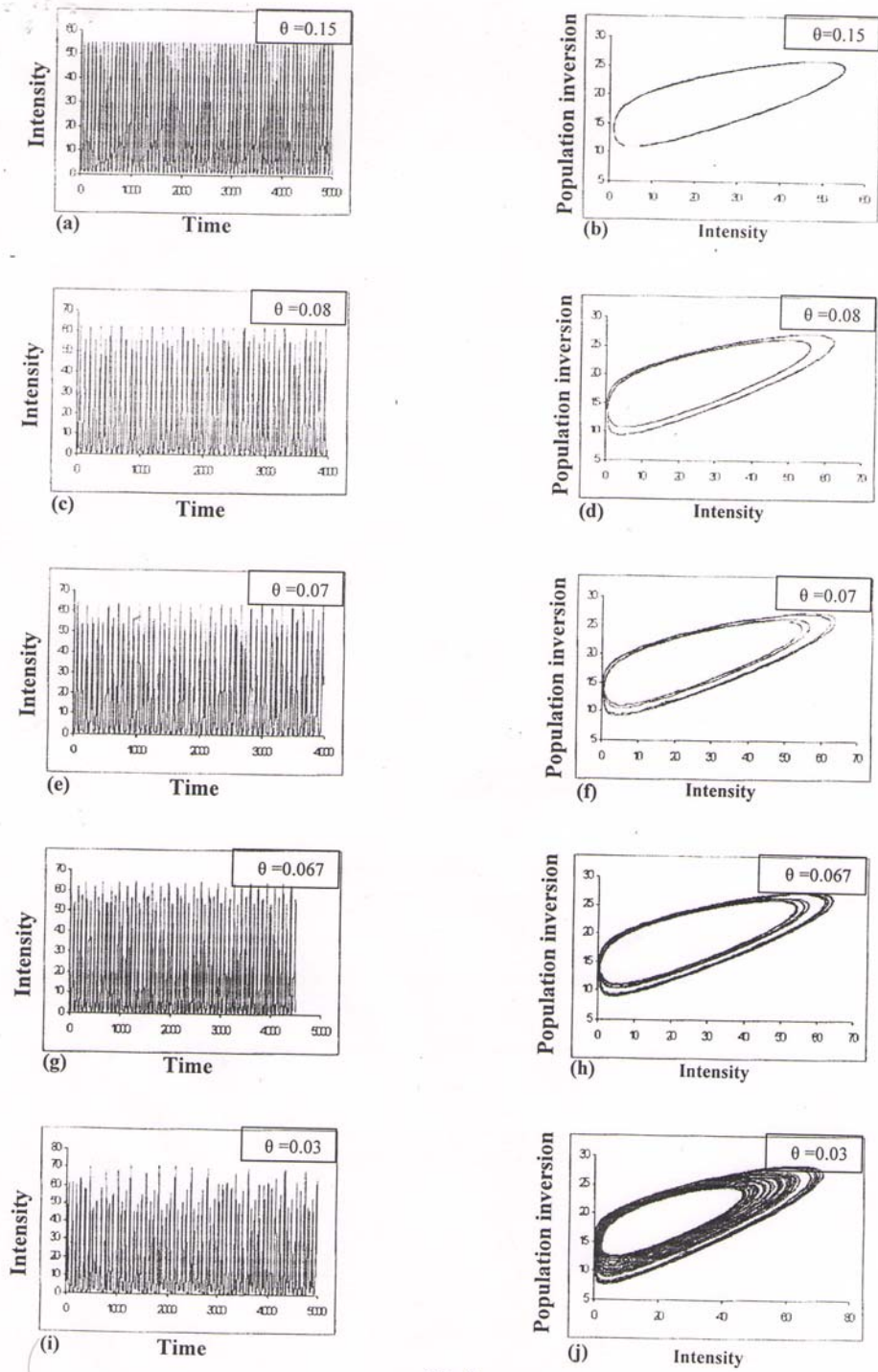


Fig.3

Fig.3. Same as Fig.1., but with $\alpha = 0$ for different values of θ .

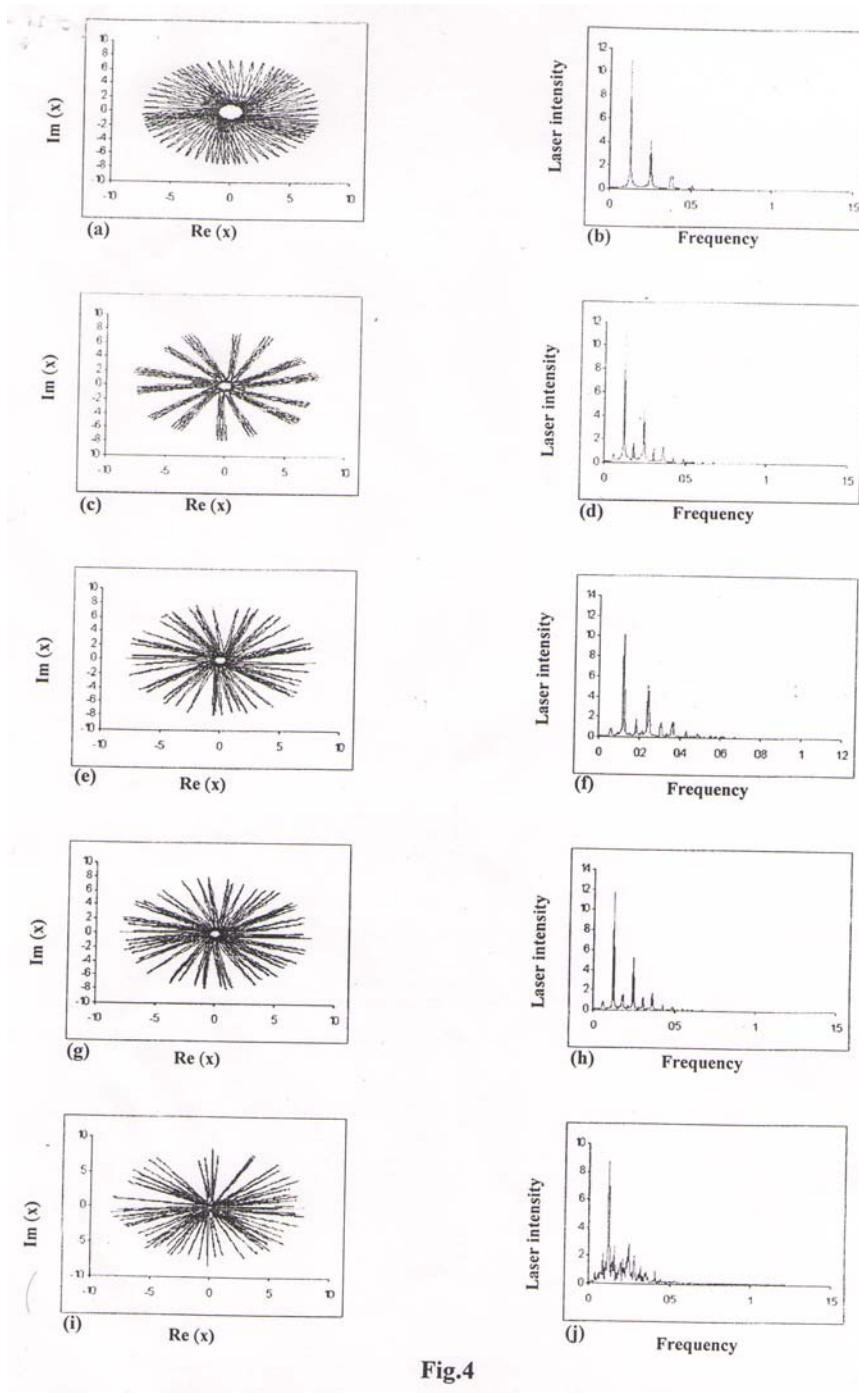


Fig.4

Fig.4. Same as Fig.2., but corresponding to the Fig.3.

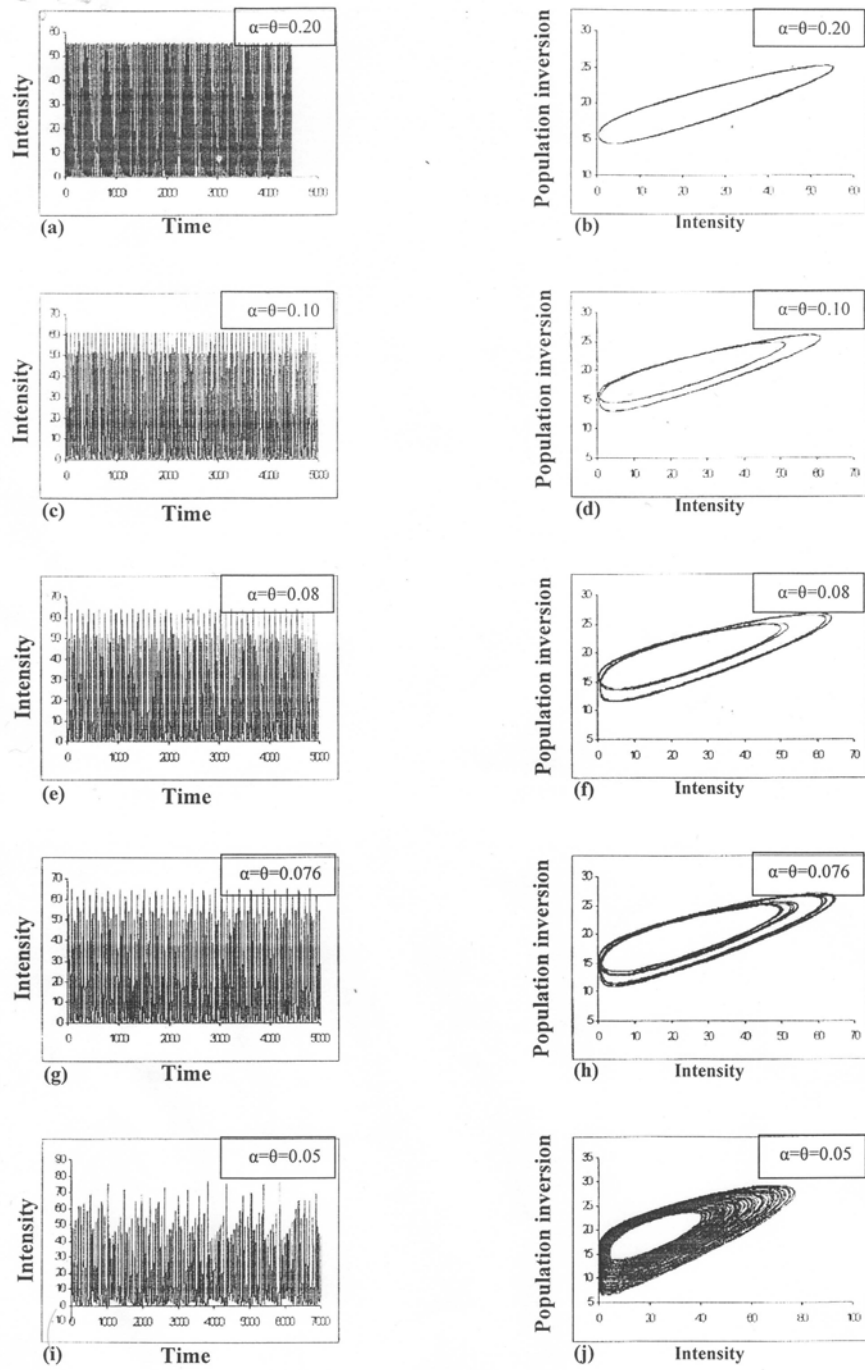


Fig.5

Fig.5. Same as Fig.1., but for different values of $\alpha = \theta$.

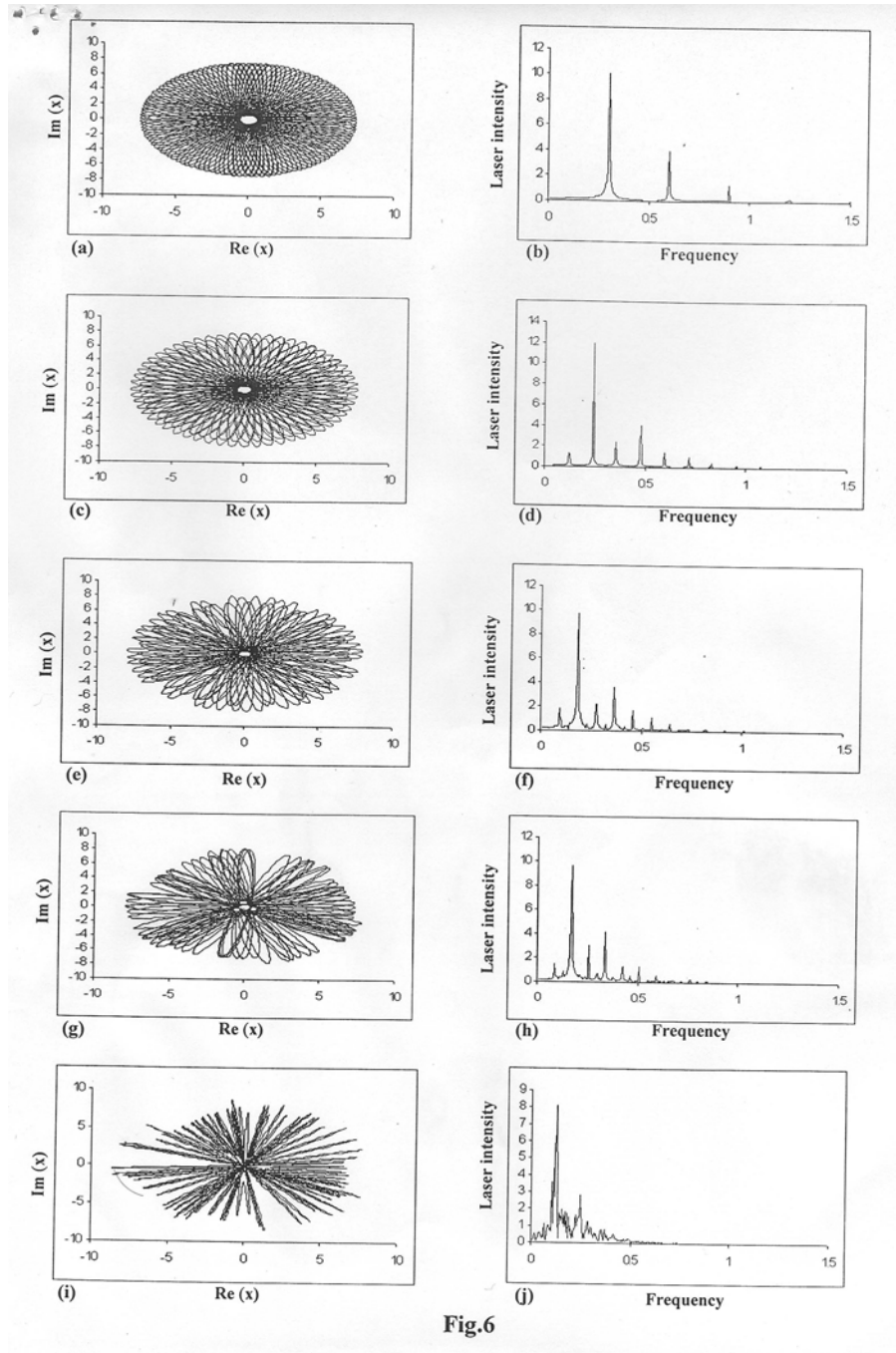


Fig.6. Same as Fig.2., but corresponding to Fig.5.